23rd ABCM International Congress of Mechanical Engineering
December 6-11, 2015, Rio de Janeiro, RJ, Brazil

SEMI-ACTIVE VIBRATION CONTROL OF A ROTATING SHAFT BY USING A MAGNETO RHEOLOGICAL DAMPER

Aldemir Ap Cavalini Jr[1]
Edson Hideki Horoishi[2]
Adriano Silva Borges[2]
Luiz Gustavo Pereira[1]
Valder Steffen Jr[1]

[1] LMEst – Laboratory of Mechanics and Structures, Federal University of Uberlândia, School of Mechanical Engineering,
Av. João Naves de Ávila, 2121, Uberlândia, MG, 38408-100, Brazil.
aacjunior@mecanica.ufu.br

[2] Federal Technological University of Paraná, Campus Cornélio Procópio, Av. Alberto Carazzai, 1640,
Cornélio Procópio, PR, 86300-000, Brazil.
edsonh@utfpr.edu.br

Abstract. *This paper is dedicated to semi-active vibration control of rotating shafts by using a magneto rheological damper as actuator. Several mathematical models were proposed in order to represent the rheological properties of this kind of actuator. However, in this work the modified Bouc-Wen model is used. A rotor composed by a horizontal flexible shaft, two rigid discs, and two self-aligning ball bearings is used to demonstrate the efficiency of the proposed control approach. A finite element model is used to obtain the numerical dynamic responses of the rotating machine. The control effort was determined using a Fuzzy Logic Control strategy as based on the Takagi-Sugeno model. The present method requires the states of the system to determine the control effort. The results of the control strategy conveyed show that the magneto rheological damper is a reliable alternative for vibration control of flexible shafts of rotating machines.*

Keywords: *rotating machines, semi-active control, magneto rheological damper, fuzzy control approach.*

1. INTRODUCTION

In recent years, a number of methods dedicated to vibration control have been proposed in order to satisfy the increasing demand for high performance and safe operation of mechanical systems. The control approaches for rotating machines are clustered into three main categories, namely passive, active, and semi-active techniques (Simões et al., 2007; Inman, 2001). Passive techniques are normally performed by devices known as absorbers or isolators. These techniques are usually effective over a limited frequency bandwidth and, consequently, are unable to adapt their characteristics to changes in the system. Differently, active approaches promise vibration suppression over a broadband frequencies in which the suppression is granted by incorporating active actuators, such as PZT stacks, magnetic bearings, and electromagnetic actuators to the machine so that they perform directly against the vibratory loads (Koroishi et al., 2014). Unfortunately, successful implementation of these approaches has been limited by displacement capabilities of the piezoelectric actuators and the expensive costs of magnetic bearings (Wickramasinghe, Chen, and Zimcik, 2008). The semi-active techniques represent an alternative solution to these problems. In semi-active approaches, the vibration is attenuated through an indirect manner by changing the structural parameters of the machine, such as damping and/or stiffness. Nowadays, the implementation of this technique in rotor dynamics is made possible by techniques such as electro rheological and magneto rheological dampers (MR dampers).

In this context, this work is dedicated to semi-active vibration control of rotating shafts by using a magneto rheological damper as actuator (MR actuator). MR fluids consist on micron-sized magnetically polarizable particles dispersed in a mineral or silicone oil solution. This kind of actuator (or damper) is able to change its damping and stiffness properties when subjected to a magnetic field (i.e., the fluid becomes a semi-solid and exhibits viscoplastic behavior when the magnetic field is applied). According to Lai and Liao (2002), the MR actuators present high strength, good stability, broad operational temperature range, and fast response time (interesting for control applications).

Therefore, this paper presents a numerical simulation approach to evaluate the effectiveness of MR actuators to attenuate high vibration amplitudes of a rotating machine under two different scenarios, namely a steady state operating condition, and crossing a critical speed during its transient motion. A horizontal flexible shaft, two rigid discs and three bearings compose the system under analysis. The control effort was determined by using a Fuzzy Logic Control based on Takagi-Sugeno model. Finally, numerical simulations are performed and the results obtained are discussed.

2. MAGNETO RHEOLOGICAL DAMPER

The Bouc-Wen model is extensively used for modeling the hysteresis phenomenon associated with non-Newtonian fluids (Wen, 1976). The mathematical model proposed by Spencer et al. (1997) is adopted in this work. The so-called modified Bouc-Wen model associates a viscous damper c_1 and a linear spring k_1, with the hysteretic phenomenon (*Bouc-Wen*) to better describe the fast drop in the force when the piston speed of the MR actuator is zero. The modified Bouc-Wen model is presented by Fig. 1.

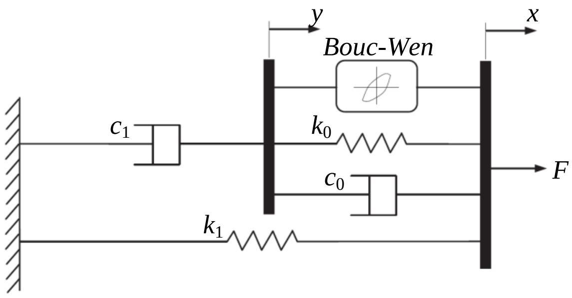

Figure 1. Modified Bouc-Wen model (Spencer et al., 1997).

The phenomenological model is governed by the following equations (Lai and Liao, 2002):

$$
\begin{aligned}
&F = c_1 \dot{y} + k_1 \left(x - x_0 \right) \\
&\dot{y} = \frac{1}{c_0 + c_1} \left[\alpha z + k_0 \left(x - y \right) + c_0 \dot{x} \right] \\
&\dot{z} = -\gamma \left| \dot{x} - \dot{y} \right| \left| z \right|^{n-1} z - \mu \left(\dot{x} - \dot{y} \right) \left| z \right|^{n} + A \left(\dot{x} - \dot{y} \right) \\
&\alpha = \alpha_a + \alpha_b u \qquad c_1 = c_{1a} + c_{1b} u \\
&c_0 = c_{0a} + c_{0b} u \qquad \dot{u} = -\eta \left(u - v \right)
\end{aligned}
\tag{1}
$$

where v is the voltage applied on the current driver of the MR actuator. Note that there are 14 parameters required to describe the MR damper. In Lai and Liao (2002), these parameters where determined by using experimental data obtained from the actuator RD-1005-1 (manufactured by Lord Corporation®). Table 1 shows the parameters for the model considered in this work.

Table 1. Parameters determined for the MR actuator RD-1005-1 (Lai and Liao, 2002).

Parameter	Value	Parameter	Value
c_{0a}	784 Ns/m	α_a	12441 N/m
c_{0b}	1803 Ns/Vm	α_b	38430 N/Vm
c_{1a}	14649 Ns/Vm	γ	136320 m^{-2}
c_{1b}	34622 Ns/Vm	μ	2059020 m^{-2}
k_0	3610 N/m	A	58
k_1	840 N/m	n	2
x_0	0.0245 m	η	190 s^{-1}

Figure 2a shows the behavior of the force F developed by the representative MR actuator (see Tab. 1) considering the following sets of displacement/voltage (x/v – mm/voltage): 0.002/2, 0.004/1.5, 0.006/1, 0.008/0.5, and 0.010/0 (Paschoal, 2011). The displacements are sinusoidal with 1 Hz frequency. The behavior of the force F versus velocity $\dot{x}$ is also presented (Fig 2b).

3. CONTROL APPROACH

Figure 3 shows the control strategy as proposed by Der Hagopian and Mahfoud (2010). Regarding the computational implementation of the fuzzy logic approach, the first step consists in the fuzzification of the states q

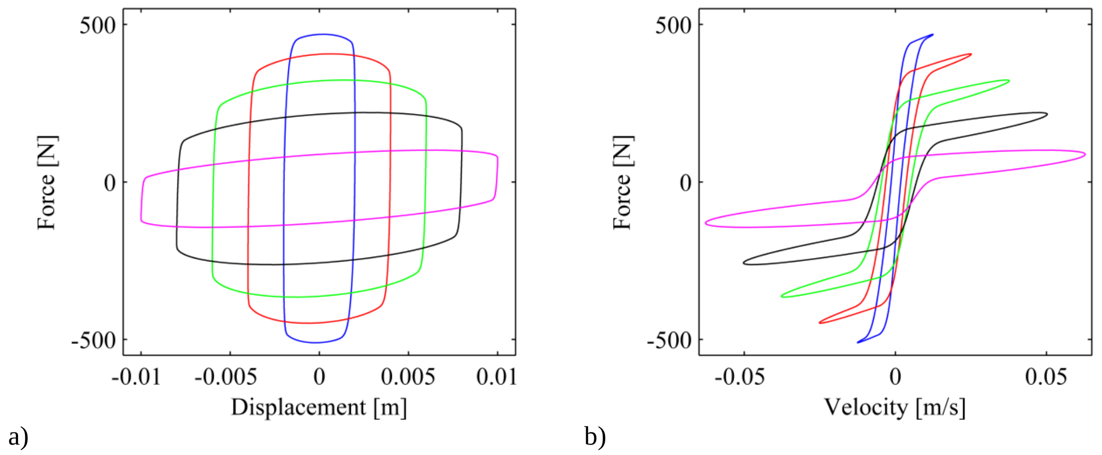

Figure 2. Behavior of the force F developed by the representative MR actuator
(x/v – mm/voltage; — 0.002/2; — 0.004/1.5; — 0.006/1; — 0.008/0.5; — 0.010/0).

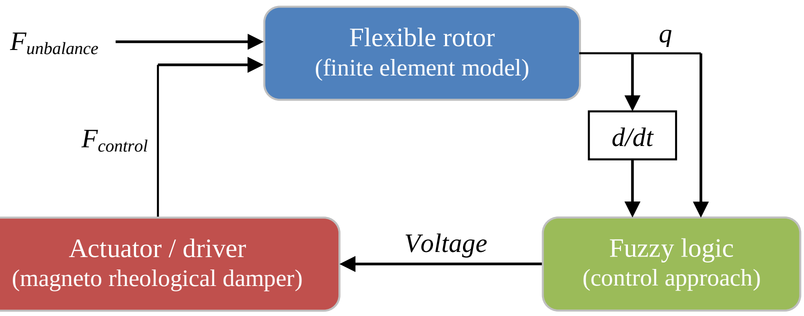

Figure 3. Control strategy ($F_{unbalance}$: unbalance force; $F_{control}$: control effort = F in Fig. 1).

(lateral displacements and velocities of the rotating shaft). The states are converted into several fuzzy variables, in which the number of variables depends on the number of membership functions used. In this work, two-membership functions were used, obtained from the GBELL Matlab® "positive" and "negative" functions (Fig.4).

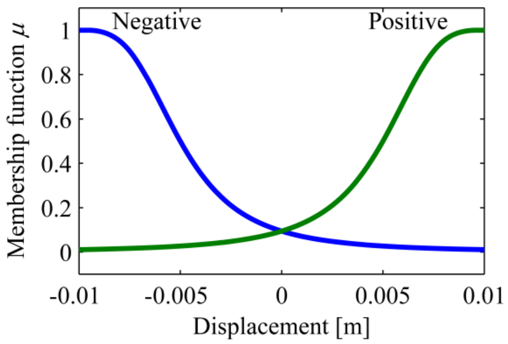

Figure 4. Input membership functions.

The inference engine implements the "minimum" function w_j. Mahfoud and Der Hagopian (2011) presented fuzzy controller rules as applied to flexible structures. These rules were used in the present contribution and they are presented in Tab. 2. The Fuzzy rules took into account two situations: "action" (i.e., application of the control effort) - when the measured displacements and velocities assume a positive or negative values, and "no action" - for the displacements and velocities presenting positive and negative or negative and positive values, respectively.

Finally, the control command is obtained after defuzzification, which requires the knowledge of the fuzzy output variables corresponding to the rules together with the aggregation of these rules (as well as the output membership functions). In this paper the Takagi-Sugeno method is used due to its good adaptation to the real time computation controller. The membership functions are presented in Eq. (2).

Table 2. Fuzzy controller rules.

Rule	Condition	Decision
1	IF positive displacement AND positive velocity	Action
2	IF positive displacement AND negative velocity	No action
3	IF negative displacement AND positive velocity	No action
4	IF positive displacement AND negative velocity	Action

$$z_1 = 0\,, \qquad z_2 = 100\delta + 1000\dot{\delta} \tag{2}$$

where z_1 corresponds to "no action" and z_2 to "action" configurations. The command voltage (Fig. 5) is given by the output of the controller and can be written as

$$F = \sum_{j=1}^{2} w_j z_j \Big/ \sum_{j=1}^{2} w_j \tag{3}$$

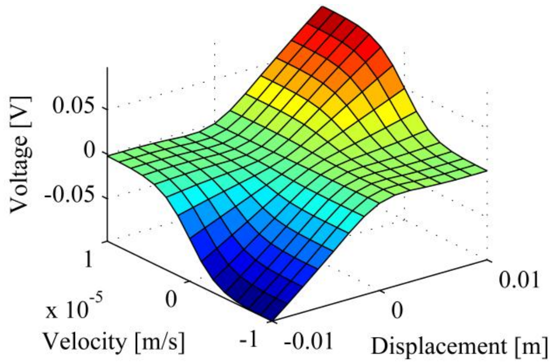

Figure 5. Fuzzy controller surface.

4. ROTOR TEST RIG

Figure 6a shows the rotor test rig used as a reference for the studied rotor model. The system is mathematically represented by 33 Timoshenko beam elements (FE model; Fig. 6b). A flexible steel shaft with 860 mm length and 17 mm of diameter (E = 205 GPa, ρ = 7850 kg/m^3, υ = 0.29), two rigid discs D_1 (node #13; 2,637 kg; according to the FE model) and D_2 (node #23; 2,649 kg), being both of steel, with 150 mm of diameter and 20 mm of thickness (ρ = 7850 kg/m^3), and two roller bearings (B_1 and B_2, located at the nodes #4 and #31, respectively) compose the rotor system. Displacement sensors are orthogonally mounted at nodes #8 (S_{8X} and S_{8Z}) and #28 (S_{28X} and S_{28Z}) to collect the shaft vibration. The system is driven by an electric DC motor.

Equation 4 presents the equation of motion that governs the dynamic behavior flexible rotor supported by roller bearings (Lalanne and Ferraris, 1998).

$$M\ddot{q} + \left[D + \Omega D_g\right]\dot{q} + \left[K + \dot{\Omega} K_{st}\right] q = W + F_{unbalance} + F_{control} \tag{4}$$

where M is the mass matrix, D is the damping matrix, D_g is the gyroscopic matrix, K is the stiffness matrix, and K_{st} is the stiffness matrix resulting from the transient motion. All these matrices are related to the rotating parts of the system, such as couplings, discs, and shaft. W stands for the weight of the rotating parts, $F_{unbalance}$ represents the unbalance forces and $F_{control}$ represents the control effort applied in the rotor by the magneto rheological actuators.

A model updating procedure was used in order to obtain a representative FE model for the numerical simulations presented on this work (Fig. 6b). For this aim, a heuristic optimization technique (Differential Evolution; Storn and Price, 1995) was used to determine the unknown parameters of the model. Therefor, the stiffness and damping coefficients of the bearings, the proportional damping added to D (coefficients γ and β; $D_p = \gamma\, M + \beta\, K$), and the stiffness k_{ROT} due to the coupling between the electric motor and the shaft (added around the orthogonal directions X and Z of the node #1) were determined. The entire frequency domain process was performed 10 times, considering 100 individuals in the initial population of the optimizer. Fig. 6b summarizes the parameters determined in the end of the minimization process associated with the smaller fitness value.

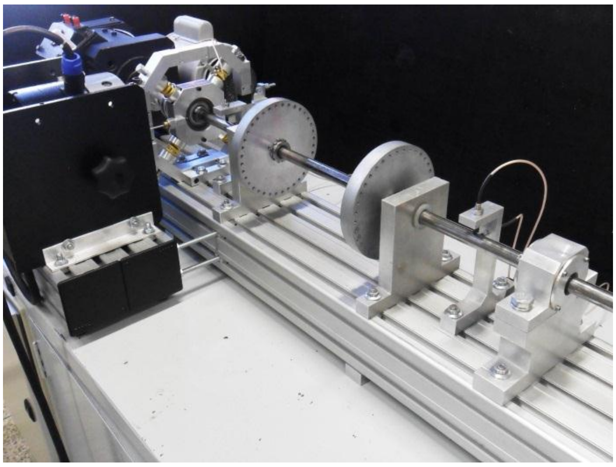

a)

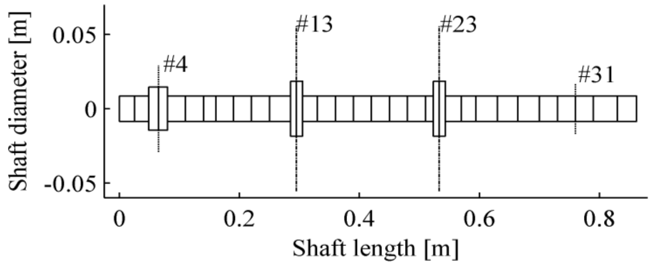

$k_{X/B1} = 8.551 \times 10^5$ $k_{X/B2} = 5.202 \times 10^7$ $\gamma = 2.730$
$k_{Z/B1} = 1.198 \times 10^6$ $k_{Z/B2} = 7.023 \times 10^8$ $\beta = 4.85 \times 10^{-6}$
$d_{X/B1} = 7.452$ $d_{X/B2} = 25.587$ $k_{ROT} = 770.442$
$d_{Z/B1} = 33.679$ $d_{Z/B2} = 91.033$

**k*: stiffness [N/m]; *d*: damping [Ns/m].

b)

Figure 6. Rotor used in the analysis of the SHM technique: a) Test rig; b) FE model.

Figure 7a compares simulated and experimental Bode diagrams, considering the parameters shown in Fig. 6b. Note that the FRF generated from the FE model is satisfactorily close to the one measured directly on the test rig. Fig. 7b compares the experimental orbit measured by the measure plane S_8 (full acquisition time of 4 s in steps of 0.002 s, approximately) with the one determined by the updated FE model. The operational rotation speed of the rotor Ω was fixed at 1200 rev/min and an unbalance of 487.5 g.mm / 0^0 was applied at the disc D_1. Note that the responses are close, as for the previously shown Bode diagrams, thus validating the updating procedure performed. It is worth mentioning that the first twelve vibration modes of the rotor were used to generate the displacement responses.

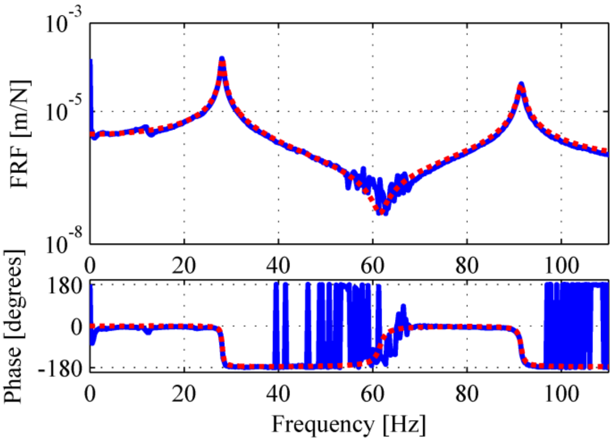

a)

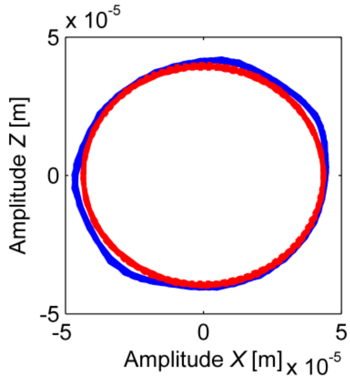

b)

Figure 7. Simulated (——) and experimental (——) Bode diagrams and orbits
(FRFs obtained from impact forces on D_1; X direction and S_{8X}).

5. NUMERICAL APPLICATION

Two situations were analyzed in terms of unbalance response. In the first case, the steady state was considered (the rotation speed is 1600 rev/min). In the second case, the transient response was studied (run-up test considering the rotation speed varying from 0 to 3000 rev/min in 20 sec). Regarding the application of the control effort, three configurations were tested. The first one (MR_{conf1}) considers the MR damper positioned along the horizontal direction of the rotor (i.e., X direction). In the second configuration (MR_{conf2}), the control effort is applied at 45 degrees with respect to the X direction. Two MR dampers were used in the third configuration (MR_{conf3}), along the X and Z directions of the rotor.

Figure 8 presents the unbalance responses for the rotor under steady state condition as obtained from the node #8 of the FE model (unbalance of 487.5 g.mm / 0^0 applied to the disc D_1). The control action on the system, in terms of vibration attenuation, can be observed for the three configurations considered: MR_{conf1} (Fig. 8a, 8b, and 8c), MR_{conf2} (Fig. 8d, 8e, and 8f), and MR_{conf3} (Fig. 8g, 8h, and 8i). Note that the best control performance was achieved by using the

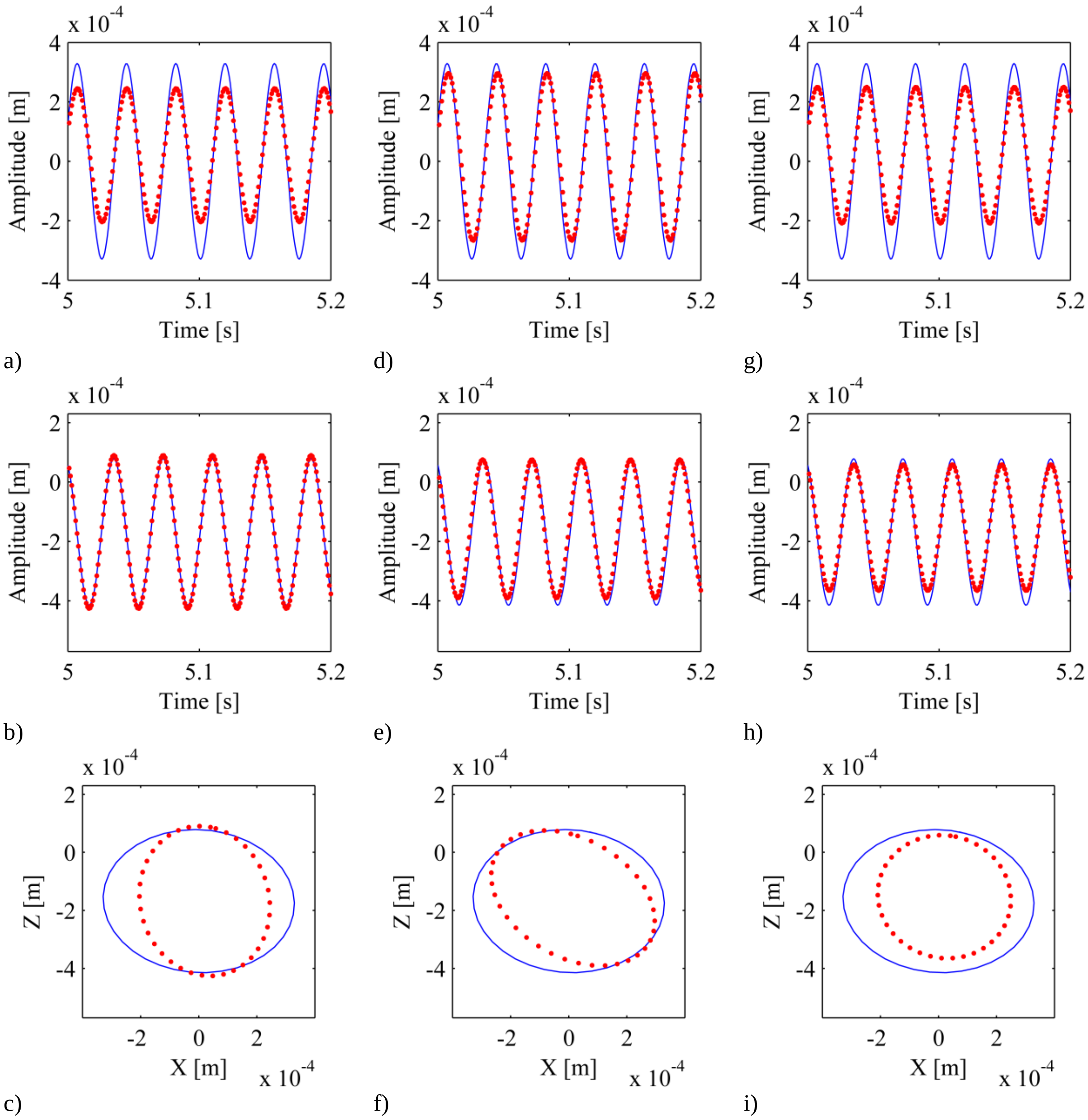

Figure 8. Uncontrolled (——) and controlled (——) vibration responses of the rotor (node #8 of the FE model).

MR_{conf3} configuration, which presented the biggest vibration attenuation along the orthogonal directions X and Z (vibration reduction of 31.8% and 12.1%, respectively). Similar results were obtained for the node #28 of the FE model.

Figure 9 shows the voltage and the associated control effort applied by the MR dampers for the three configurations: MR_{conf1} (Fig. 9a and 9b), MR_{conf2} (Fig. 9c and 9d), and MR_{conf3} (Fig. 9e and 9f). Considering MR_{conf3}, note that the voltage and control force required by the MR damper positioned along the X direction are different of the ones determined for the MR damper positioned along the Z direction (i.e., along the Z direction there is the influence of gravity).

Figure 10 shows the vibration attenuation for the rotor crossing the first critical speed along the two perpendicular directions from node #8 of the FE model (Fig 10a: X direction; Fig 10b: Z direction). Only the configuration MR_{conf3} was evaluated, in which an unbalance of 487.5 g.mm / 0^0 was applied at the disc D_1. Additionally, the voltage and the associated control effort applied in the MR dampers are shown (Fig. 10c and 10 d, respectively). Considering the rotation at the critical speed (i.e., 1780 rev/min), the vibration amplitude along the X direction was reduced in 37.6%. Along the Z direction, the vibration reduction was 6.4%. Figures 10c and 10d present the voltage and the associated control effort applied by the MR dampers for the MR_{conf3} configuration. Similar results were obtained for the node #28 of the FE model.

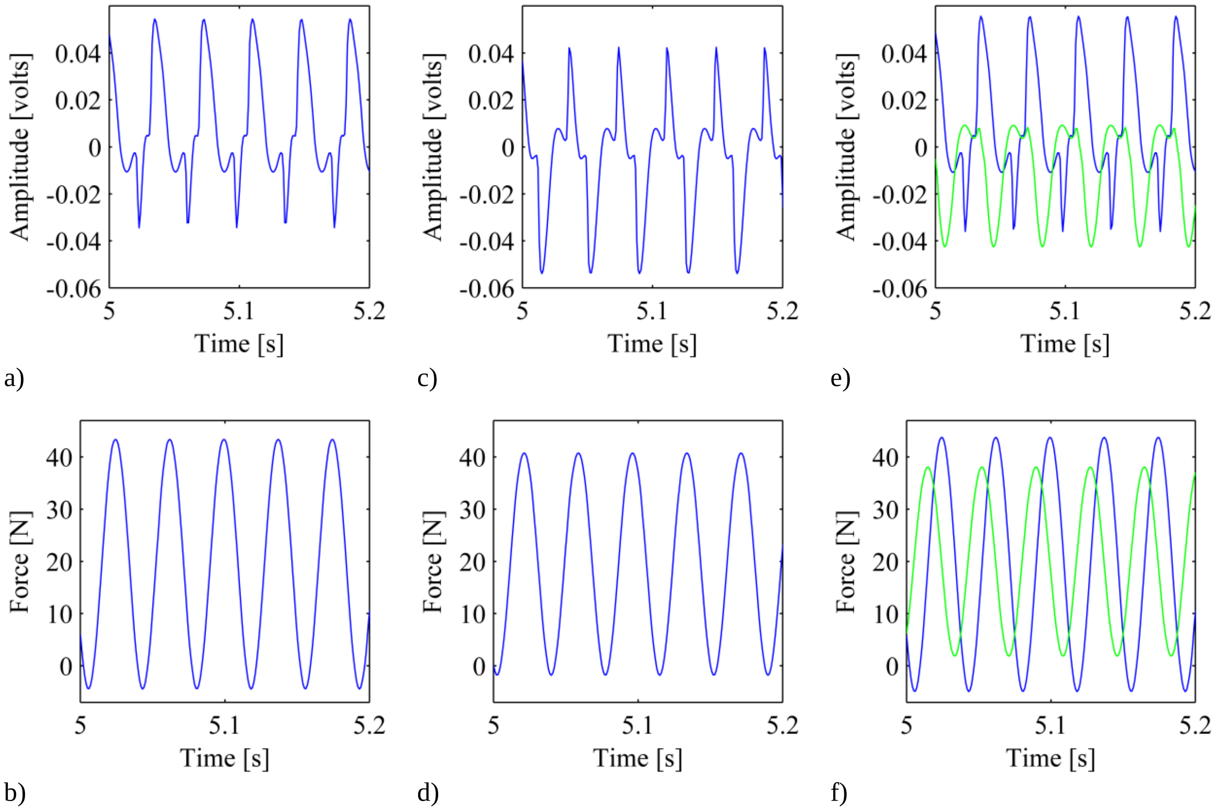

Figure 9. Voltage and the associated control effort applied by the MR dampers for the three configurations (Fig. 9e and 9f: —— MR actuator along the *X* direction; —— MR actuator along the *Z* direction).

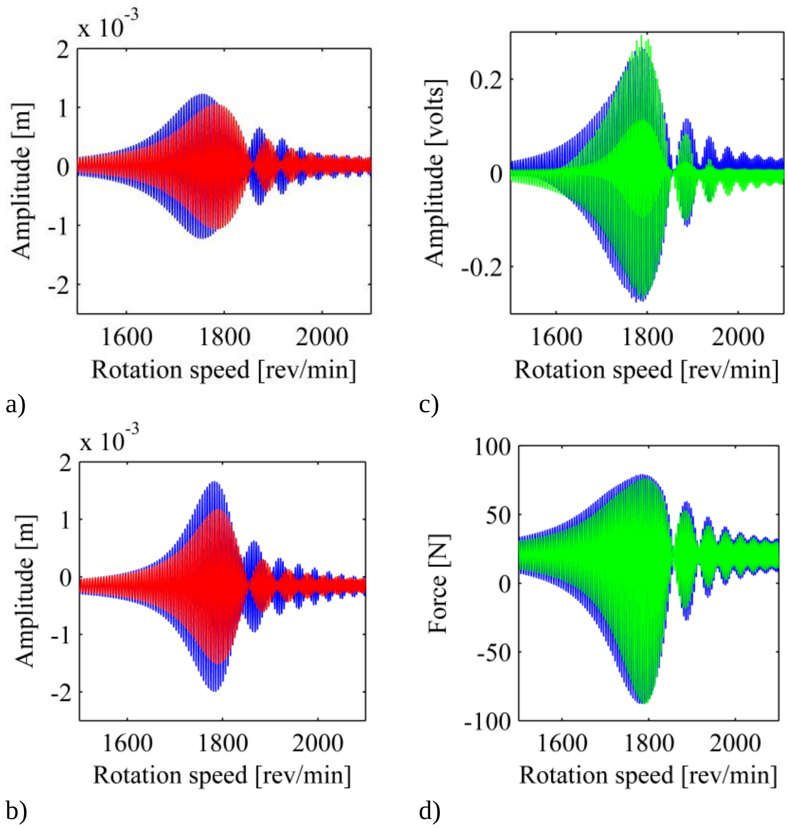

Figure 10. Uncontrolled (——) and controlled (——) vibration responses of the rotor (Fig 10a and 10b). (Fig. 10c and 10d: —— MR actuator along the *X* direction; —— MR actuator along the *Z* direction).

6. CONCLUSIONS

In this paper, a control approach was successfully applied to a complex rotor system using magneto rheological dampers. Three configurations of MR dampers were associated with a Fuzzy logic based strategy to attenuate the lateral vibration of a flexible rotor. Numerical results showed that the proposed methodology was efficient considering the rotor under two operating conditions, namely steady state response for constant rotation speed, and run-up test (i.e., transient response). The steady state and transient unbalance responses were reduced about 30% regarding the vibration amplitude along the X direction and 10% considering the response determined along the Z direction (Z coincides with the direction of gravity). The numerical tests seem to be interesting since they can be used to adjust the controller and the FE model of the system for further experimental applications. Therefore, further research work will encompass experimental evaluations of the proposed control methodology.

7. ACKNOWLEDGEMENTS

The authors are thankful to the Brazilian Research Agencies FAPEMIG and CNPq (INCT-EIE) and also to CAPES for the financial support provided for this research effort.

8. REFERENCES

Der Hagopian, J. and Mahfoud, J., 2010, “Electromagnetic Actuator Design for the Control of Light Structures”. S*mart Structures and Systems*, Vol. 6, p. 29-38.

Mahfoud J. and Der Hagopian, J., 2011, “Fuzzy Active Control of Flexible Structures by Using Electromagnetic Actuators”. *Journal of Aerospace Engineering*, Vol. 24, p. 329-337.

Lalanne, M. and Ferraris, G., 1998, “Rotordynamics Prediction in Engineering”. John Wiley & Sons.

Storn, R. and Price, K., 1995, “Differential Evolution: A Simple and Efficient Adaptive Scheme for Global Optimization over Continuous Spaces”. *International Computer Science Institute*, Vol. 12, p. 1-16.

Simões, R.C., Steffen Jr., V., Der Hagopian, J., and Mahfoud, J., 2007, “Modal Active Vibration Control of a Rotor Using Piezoelectric Stack Actuators”. *Journal of Vibration and Control*, Vol. 13, p. 45-64.

Inman, D.J., 2001, “Engineering Vibration”, Prentice-Hall, Upper Saddle River, NJ, USA.

Wickramasinghe, V., Chen, Y., and Zimcik, D., 2008, “Experimental Evaluation of the Smart Spring Impedance Control Approach for Adaptive Vibration Suppression”. *Journal of Intelligent Material Systems and Structures*, Vol. 19, p. 171-179.

Koroishi, E.H., Borges, A.S., Cavalini Jr, A.A., and Steffen Jr, V., 2014, “Numerical and Experimental Modal Control of Flexible Rotor Using Electromagnetic Actuator”. *Mathematical Problems in Engineering*, Vol. 2014, p. 1-14.

Spencer Jr., B.F. , Dyke, S.J., Sain, M.K., and Carlson, J.D., 1997, “Phenomenological Model of a Magnetorheological Damper”. *ASCE Journal on Engineering Mechanics*, Vol. 123, p. 230-238.

Wen, Y.K., 1976, “Method of Random Vibration of Hysteretic Systems”. *ASCE Journal on Engineering Mechanics*, Vol. 102, p. 249-263.

Lai, C.Y. and Liao W.H., 2002, “Vibration Control of a Suspension System via a Magnetorheological Fluid Damper”, Journal of Vibration and Control, *Vol.* 8, p. 527-547.

Paschoal, E.F., 2011. *Controle semi-ativo de vibrações usando lógica nebulosa e fluido magnetoreológico*. Master’s Thesis. Faculdade de Engenharia de Ilha Solteira, Ilha Solteira, SP, Brazil.

9. RESPONSIBILITY NOTICE

The authors are the only responsible for the printed material included in this paper.